

# Research Journal of Pharmaceutical, Biological and Chemical Sciences

## Physicochemical Analysis of Structure of Foamed Concrete with Addition of Oil Sludges.

K. A. Bissenov\*, S. S. Uderbayev, and N. A. Saktaganova.

Korkyt Ata Kyzylorda State University, st. Aiteke 29A, Kyzylorda, The Republic of Kazakhstan, 120014.

### ABSTRACT

The article discusses the results of investigation into physicochemical properties of individual phases, cementing bond of foamed concretes. Physicochemical variations of macro- and microstructure of foamed concrete on the basis of fine multi-component dry mixtures with the use of oil sludges are analyzed.

**Keywords:** foamed concrete, surfactant, oil sludge, cellular structure, macrostructure, microstructure.

*\*Corresponding author*

## INTRODUCTION

The issues of resource and energy saving, as well as of environmental safety require for solution of some important problems, including development and production of heat insulating materials. The necessity of technology development of non-autoclaved concretes in construction industry is stipulated by high demand for efficient construction materials. The main consumer requirements, in addition to low density and high strength of materials, are low cost of products and ease of fabrication. The most efficient heat insulating and engineering materials are cellular concretes with low coefficients of heat conductance, they are fabricated of relatively inexpensive raw stock. While autoclave technology is more efficient method of fabrication of high quality aerated concrete, it requires for high energy costs, which is not economically feasible in modern market environment. The issue of energy efficiency of buildings can be solved by means of aerated materials on the basis of gas-concrete mixtures with preset viscosity, their application would provide erection of protecting structures with preset optimum technical and economical performances [1, 2, 3]. Nowadays solution of this problem is very urgent.

At present attention is attracted to non-autoclaved aerated concrete due to relatively moderate energy consumption cost. This list of reduced expenses for fabrication of non-autoclaved concrete items includes the following procedures:

- Delivery and processing of raw stock;
- Metering of components;
- Steam treatment;
- Decrease in consumption of electricity and steam;
- Low demand in labor force;
- Reduced metal intensity of equipment.

The main reasons, which restrict wide application of non-autoclaved cellular concrete, are limited possibilities of application of raw stock, enabling fabrication of products with specified strength properties. Analysis of published research results demonstrates that non-autoclaved cellular concretes are conventionally fabricated of quartz sands and some technogenic wastes with high silica content, which stipulates their availability as silica fillers of cellular concretes. However, deposits of pure quartz sands are limited, they should be replaced with other fillers, and in this regard the technology of non-autoclaved cellular concretes on the basis of local natural and technogenic raw stock is very promising [4, 5, 6].

The issue of complex research of non-conventional silica raw stock, determination of its applicability for fabrication of non-autoclaved cellular concrete, development of its reasonable composition and fabrication of aerated concrete upon formation of porous structure and main physico-mechanical properties should be studied in details.

Peculiar feature of aerated concrete, mainly of heat insulating materials, differing it from other types of concretes, is its structure with pores, their size varies from several millimeters to tens of Angstrom, and total porosity is 20-90%.

Pores are fine cavities in material, filled with air or water. The quality of heat insulating concrete and items on its basis depend mainly on the structure of inter-pore partitions and pore space.

The notion of structure of inter-pore partitions includes structure and mineral composition, degree of solidification and dispersity of neoformations, and the structure of pore space involves quantity and quality of macro- and micro-pores and their quantitative ratio.

The properties of cellular concrete depend not only the quantitative property of porosity, but also on uniformity of pore distribution along cross section, thickness and strength of inter-pore walls, homogeneity of pores and walls.

Cellular structure stipulates both advantages and disadvantages of these concretes: increased porosity provides high heat insulating properties of the materials but reduces its strength at the same time [7, 8].

In general case the structure of concrete implies a set of steady bonds of objects providing its integrity and consistency, that is, maintaining of major properties under various external and internal changes.

The structure of pore space depends also on the type, amount of blowing agents, as well as on the method of formation of macropore structure. Sometimes the elements of structure, which hardly could be detected, significantly influence on operational properties of products. For instance, foamed concrete and aerated concrete differ only by the type of blowing agent, the first of them contains higher amount of surfactants covering solid surface with thin layer. Nevertheless, this nearly undetectable element influences on the properties of cellular concrete [9, 10].

## EXPERIMENTAL

We studied physicochemical changes of macro- and micro-structure of cellular concrete on the basis of fine multi-component dry mixtures with the use of oil sludge.

Portland cement curing is usually determined by hydration of clinker minerals  $C_3S$ ,  $\beta$ - $C_2S$ ,  $C_3A$   $C_4AF$ . The main component of Portland cement clinker, tricalcium silicate, at temperatures below  $80^\circ\text{C}$  and low W/S ratios transforms into hydrosilicate  $C_2SH_2$  with  $C/S=1.5$  and appropriate amount of  $\text{Ca}(\text{OH})_2$ . However, hydration by high amount of water leads to generation of hydrosilicate of CSH(B) family: tobermorite.

At  $80$ - $120^\circ\text{C}$  the final product of  $C_3S$  hydration is  $C_2SH(B)$ .

Another mineral of silicate component of clinker is belite, or  $\beta$ - $C_2S$  at the temperatures below  $120^\circ\text{C}$  is hydrated with formation of  $C_2SH_2$  and CSH(B) – tobermorite.

Tricalcium aluminate,  $C_3A$ , at the temperatures below  $90$ - $100^\circ\text{C}$ , being hydrated in saturated lime solution, forms hexagonal crystals of hydroaluminate  $C_4AH_{13}$ . At low CaO content in liquid phase hexagonal  $C_2AH_8$  or mixture of  $C_4AH_{13}$  and  $C_2AH_{18}$  is formed. Hexagonal calcium hydroaluminates are metastable and are transformed into isothermal crystals of tricalcium aluminate  $C_3AH_6$ .

Hydration of  $C_4AF$  up to  $250^\circ\text{C}$  leads to formation of solid solutions of  $C_3(A,F)H_6$  series, hematite and  $\text{Ca}(\text{OH})_2$ .

The rate of interaction of clinker minerals with water depends both on their individual features and on amount of tempering water, ground particle size, hydration temperature. Interaction between Portland cement and water is more complicated than that of single clinker minerals and mixtures thereof. The most obvious is the phase composition of calcium hydrosilicates generated upon curing of Portland cement. It is established that at the temperatures below  $100^\circ\text{C}$  the only silicate phase in cured Portland cement is  $C_2SH_2$ . Upon hydration of Portland cement significant amount of free lime  $\text{Ca}(\text{OH})_2$  is formed.

Alumoferrite component of hydrated Portland cement is presented by  $C_4AH_{13}$  and  $C_4FH_3$ . In the presence of gypsum ettringite  $C_3A_3 \text{Ca SO}_4H_{31}$  is generated, as well as similar sulfoferrite, which in the temperature range from  $70^\circ\text{C}$  to  $100^\circ\text{C}$  is decomposed into  $C_3A$ -  $\text{Ca SO}_4$ - $H_{12}$  and  $C_3 F^*\text{Ca SO}_4H_{12}$ , which in combination with  $C_4AH_{13}$  and  $C_4FH_{13}$  form solid solutions.

Under regular curing conditions the interaction between Portland cement and filler, even fine ground, runs very slowly, it probably can be neglected. Upon steam curing and, especially, autoclaving, Portland cement actively interacts with silica filler, which leads to variation in curing pattern. It is established that under the conditions of hydrothermal processing upon interaction of  $C_3S$  and  $\beta$ - $C_2S$  with  $\text{SiO}_2$  of sand instead of dicalcium hydrosilicates, forming low strength crystalline aggregations, there appear fibrous and lamellar hydrosilicates of CSH(B) series: tobermorite. The higher is their amount, the higher is the strength of product. In addition, addition of sand accelerates silicate hydration, as well as total amount of neoformations increases. Therefore, upon hydration with autoclaving of Portland cement--silica filler we should expect occurrence of the following neoformations: hydrosilicates  $C_2SH_2$ , CSH(B) - tobermorite, hydroaluminate  $C_3AH_6$ , calcium sulfoaluminates, Portlandite, carbonates (generated in time - upon carbonization of hydrosilicates and Portlandite by air carbon dioxide, or can be added with silica component).

Identification of hydrate neoformations in cured aerated concretes by X-ray patterns is hindered due to the fact that their lines are overlapped by the lines of clinker grains and silica components.

Derivatographic analysis also does not provide complete information about phase composition of cement stone, since together with the phases experiencing physical and chemical transformation upon heating, running with evolution or absorption of heat (for instance, dehydration, polymorphic transformations and others), the considered samples can contain thermoamorphous phases in the range of operation temperatures of device.

Hence, physicochemical properties of concrete samples should be analyzed by X-ray phase, derivatographic and petrographic methods in combination.

*Investigation into physicochemical properties of individual phases, cementing bonds of concretes.*

CSH(B) is the partially solidified tobermorite-like calcium hydrosilicate with varied ratio  $\text{CaO/SiO}_2$  and varied amount of water.

The study of CSH(B) demonstrated its similarity with lamellar minerals of selling clays. It includes the ability of reversible return of certain amount of water contained between the layers of crystalline lattice, which is accompanied by variation of the distance between these layers in the range of 9.3-14Å: increase in water content leads to increase in the distance between the layers. The basicity of hydrosilicates of CSH(B) series can vary in the range of 0.8--1.5, herewith, the existence of four individual phases was established:  $\text{C}_4\text{S}_5\text{aq}$ ,  $\text{CSaq}$ ,  $\text{C}_5\text{S}_4\text{aq}$ , and  $\text{C}_4\text{S}_3\text{aq}$ . These phases cannot be distinguished by X-ray analysis. The main difference is revealed in DTA curves:  $\text{C}_{48}$  provides exothermic effect at 900°C,  $\text{C}_5\text{S}_4\text{aq}$  at 860°C,  $\text{CSaq}$  и  $\text{C}_4\text{S}_5\text{aq}$  at 830°C, however, the effect of  $\text{CSaq}$  is twice as much as that of  $\text{C}_4\text{S}_5\text{aq}$ . This effect accompanies transition of dehydration products of CSH(B) into  $\beta$ -wollastonite. Thermogravimetric curves have no sharp kinking, upon heating CSH(B) uniformly losses water in the range of 20-500°C or 20-700°C.

In microscope CSH(B) is presented by colorless fibrous crystals, rolled into foils, in electron microscope -- by fibers or twist foils.

Tobermorite 11.3Å is the main component of binder of numerous autoclaved cement-silica and lime-silica products.

In electron microscope tobermorite 11.3Å is of the form of flat lamellas or plates, usually octahedral, less often of fibers.

The structure of lamellar tobermorite is very close to that of fibrous hydrosilicates of CSH(B) series. The difference between them is that in CSH(B) the tobermorite lamellas are twisted into tubes. Tobermorite is considered as well solidified CSH(B).

Diffraction pattern of tobermorite is characterized by splitting of 3.03Å line, peculiar for fibrous hydrosilicates in lines 2.96 and 3.07 Å.

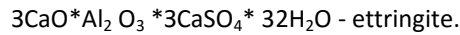
Basicity of synthetic tobermorite can vary from 0.8 to 1.25. Its thermogram provides endothermic effect at 230-260°C (dehydration). Exothermal effect of wollastonite solidification is not detected or weakly manifested at 830-850°C.

$\text{C}_2\text{SH}_2$  is the partially solidified tobermorite-like calcium hydrosilicate with the ratio  $\text{CaO/SiO}_2$  from 1.5 to 2. In microscope it is of the form of fibers or corrugated plates, in electron microscope --of the form of fibers, fiber bunches with split or contracted edges, twisted foil. The thermogram shows endothermic effect at 120-150°C, which accompanies dehydration, no other thermal effects.

$\text{C}_2\text{SH}/(\text{B})$  can have variable composition in the range of  $\text{C}1.75\text{-}2.4\text{SH}1.1\text{-}1.5$ . The thermograms of  $\text{C}_2\text{SH}(\text{B})$  show endothermic effect at 540-560°C, according to other data at 540-630°C, occurring with weight loss. The shape of crystals is fibrous or prismatic. In electron microscope -- fibrous or needle-like crystals of small size forming clusters.

Afwillite —  $3\text{CaO} \cdot 2\text{SiO}_2 \cdot 3\text{H}_2\text{O}$ . In microscope - colorless elongated prismatic crystals, in electron microscope -- prismatic. Steady phase in  $\text{CaO-SiO}_2\text{-H}_2\text{O}$  family at  $110\text{-}160^\circ\text{C}$ . The DTA curve shows three endoeffects at  $240$ ,  $320$ , and  $470^\circ\text{C}$  (dehydration) and exoeffect at  $820^\circ\text{C}$  (generation of  $\text{C}_3\text{S}_2$  or  $\beta\text{-C}_2\text{S}$ ), according to other data - endoeffect at  $370\text{-}400^\circ\text{C}$  (dehydration) and exoeffect at  $800\text{-}850^\circ\text{C}$  (solidification).

$\text{C}_3\text{AH}_6$  - In microscope, colorless globular grains, octahedra, rhombic dodecahedra. In the thermogram significant endothermic effect at  $330\text{-}340^\circ\text{C}$  corresponds to removal of  $\sim 4.5$  water molecules and weaker effect at  $500\text{-}520^\circ\text{C}$  to removal of remaining  $1.5$  water molecules.



Colorless needle-like crystals or elongated prisms, often collected into spherulites. In electronic microscope needle-like crystals, spherulites, often rather thick rods or plates, sometimes with sharp cut edges, can be observed. The thermogram shows endothermic effect at  $100\text{-}200^\circ\text{C}$  (maximum at  $150^\circ\text{C}$ ), accompanying dehydration. It is generated at early hydration stages of Portland cement.

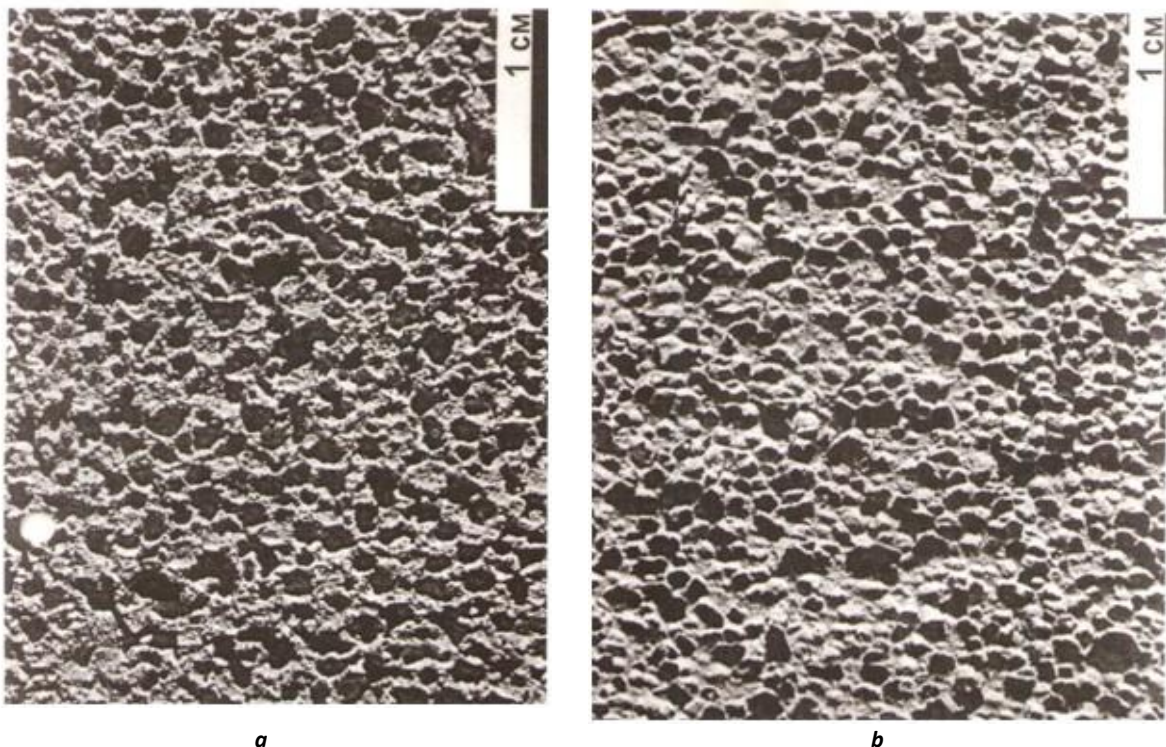
$3\text{CaO} \cdot \text{Al}_2\text{O}_3 \cdot \text{CaSO}_4 \cdot 12\text{H}_2\text{O}$  is the low sulfate form of calcium hydrosulfoaluminate. It is solidified in the form of colorless hexagonal plates, often collected into spherulite groups or stellar aggregates. In electron microscope: plates of prismatic habitus and hexagonal tablets. The thermogram shows several endothermic effects of dehydration:  $100$ ;  $150$ ;  $190\text{-}200$ ;  $300\text{-}320^\circ\text{C}$ ; according to other data:  $100\text{-}200$ ;  $200\text{-}300$  (high);  $300\text{-}320$  and  $500^\circ\text{C}$  and moderate exothermic effect at  $800^\circ\text{C}$ .

$\text{Ca}(\text{OH})_2$  is the Portlandite. Crystals are of the form of basal plates. The DTA curve shows endothermic effect of dehydration at  $585^\circ\text{C}$ , according to other data at  $480\text{-}520^\circ\text{C}$ .

$\text{CaCO}_3$  is the calcite. Colorless rhombohedra. The thermogram shows endothermic effect of dissociation into  $\text{CaO}$  and  $\text{CO}_2$  at  $860\text{-}1100^\circ\text{C}$ , sometimes double occurrence (dissociation of secondary and primary calcite, respectively).

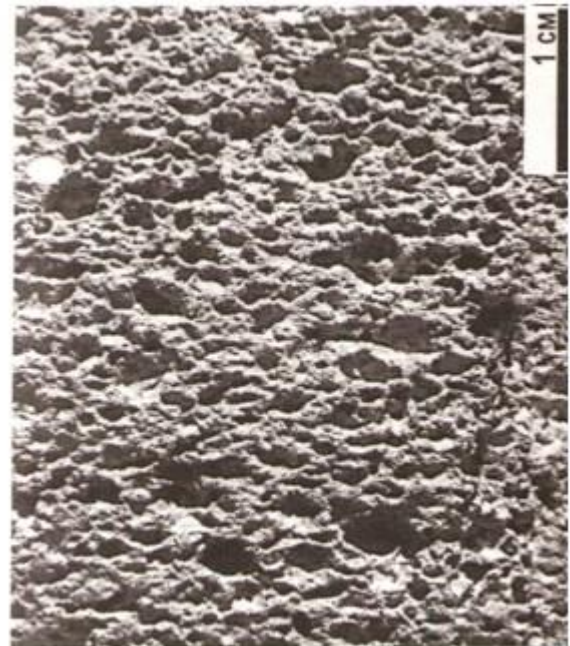
The results of alteration of structure of aerated concrete on the basis of fine dry mixtures with oil sludge were obtained in engineering laboratory.

Figures 1 and 2 illustrate macro- and micro-structures of the samples.





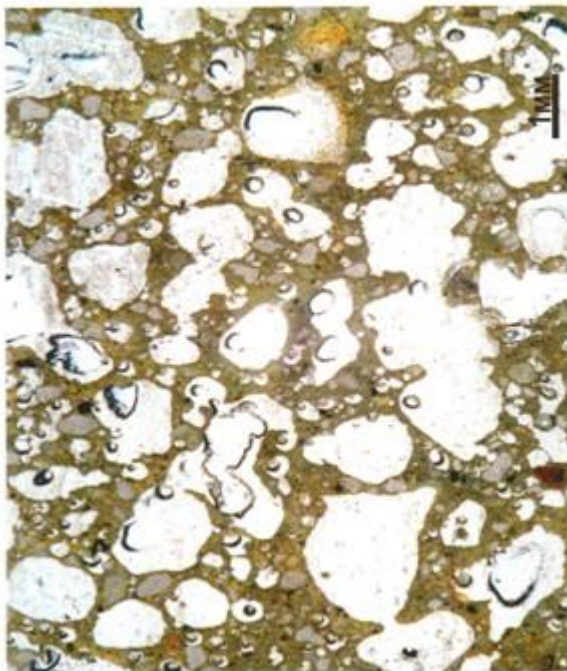
*c*



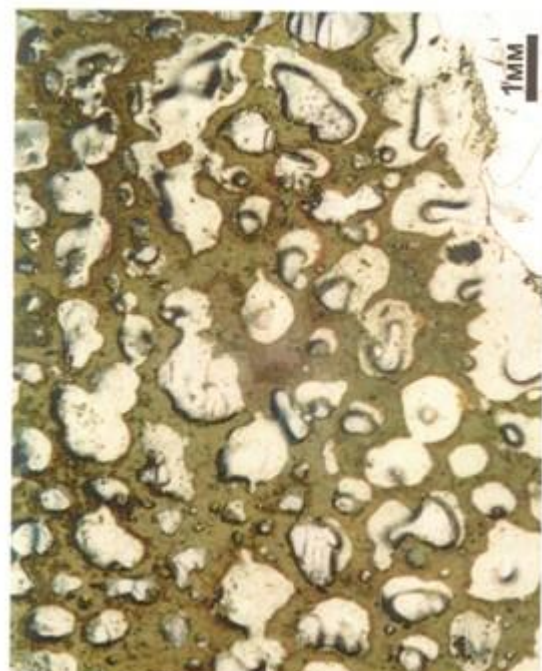
*d*

**Fig.1 Macrostructure of foamed concrete.**

*a – sample No. 1; b – sample No. 2; c – sample No. 3; d – sample No. 4.*



*a*



*b*

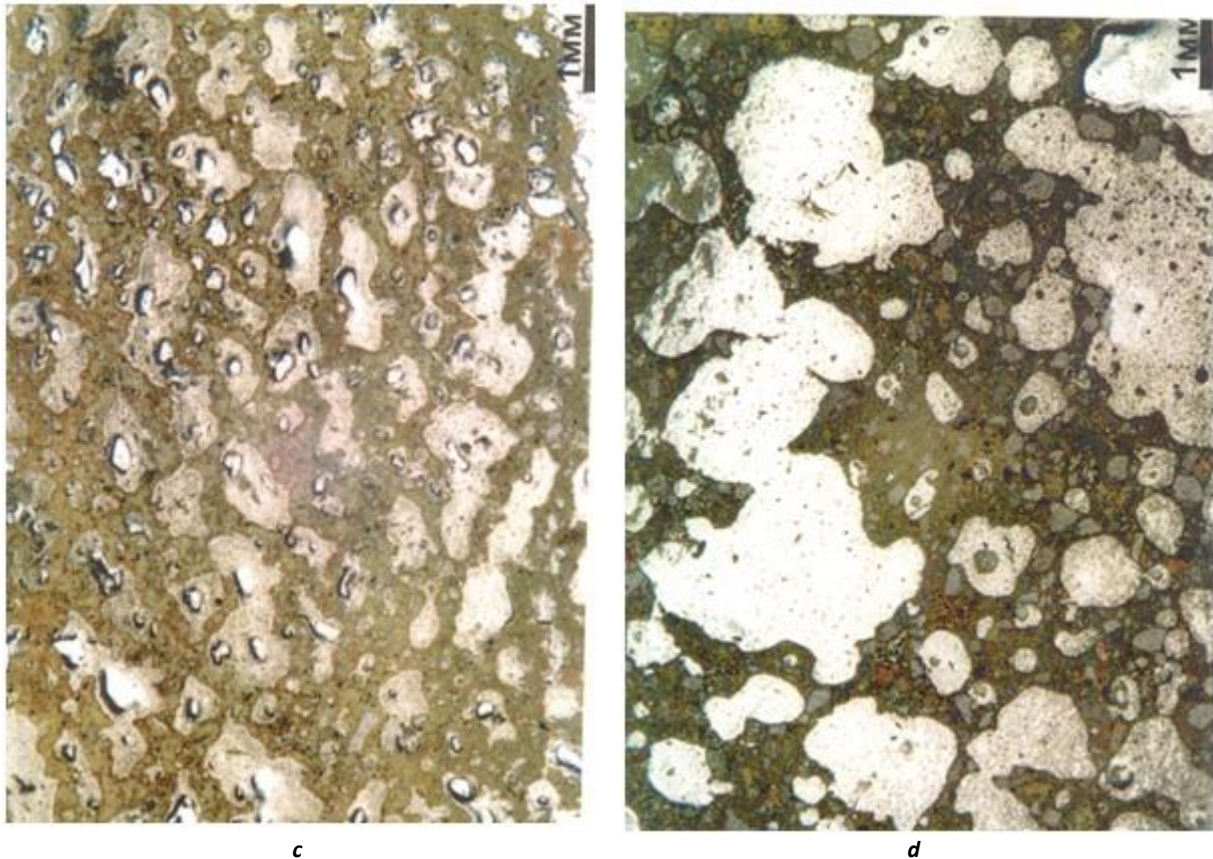


**Fig. 2. Microstructure of foamed concrete.**

***a – sample No. 1; b – sample No. 2; c – sample No. 3; d – sample No. 4.***

Regular barchans sand contains extreme amount of rocks fragments in additional to single minerals, weak roundness of numerous grains, weak grading of rocks fragments. Samples Nos. 1 and 2 are characterized by formation of well devitrified crust of Portlandite (the length of tabular crystals up to 0.1 mm).

Sample No. 1 is characterized by inert filler, sand, the sized of fragmented grains = 0.5-0.2 mm, the latte rare predominant. The grain composition: quartz, microquartzite, feldspar, single shale fragments, main effusive rocks, amphibole, limestone.

Cementing paste: hydrated paste of cement stone is comprised of:

- Fine crystalline neoformations: aggregates of fine calcite grains, at the interface only crystals of calcium oxide hydrate and calcite can be determined optically, in addition to crystalline components clusters of gel-like paste of brownish color are present. At the interface with gaseous voids thin margin of hydrosilicates and calcium hydroalumosilicates is formed with a brush of Portlandite crystals, in some pores of 0.01 mm in length.

For sample No. 2: inert filler, sand, the sizes and composition of fragmented grains are similar to sample No. 1, and coarser fragments of carbonate. Cementing paste is also similar in terms of composition and structure, but with more uniformly distributed and smaller gas generated pores. At the interface with pores neoformations similar to sample No. 1 in terms of composition and size, though, wider and better devitrified ones can be more often observed. Reactive margins at the interface with filler grains are also met more often and developed more actively.

For sample No. 3 the inert filler: fragments with the sizes from 0.2 (single) to 0.03-0.05 mm (majority). The composition is similar, no polymineral grains. Reactive margins at the interface with filler grains are stable, rare inert contacts with binder. Cementing paste is similar in terms of structure to sample No. 2, but the

composition includes relatively higher amount of calcium silicates and aluminosilicates and lower amount of hydrates. At the interface with gaseous voids thin margin of calcium hydrosilicates and hydroaluminosilicates in rare cases achieves 0.01 mm, but Portlandite crystals of such sizes and in such amount as in samples Nos. 1 and 2 do not occur, and the margin is quite often not pronounced (though, this is not completely confirmed by diffractometry).

For sample No. 4 the inert filler: fragments with the sizes from 0.2 (single) to 0.03-0.1 mm (majority). The composition is similar, no polymer grains. Reactive margins at the interface with filler grains are stable, rare inert contacts with binder. Cementing paste is similar in terms of structure to sample No. 2, but the composition includes relatively higher amount of calcium silicates and aluminosilicates and lower amount of hydrates. At the interface with gaseous voids thin margin of calcium hydrosilicates and hydroaluminosilicates in rare cases achieves 0.03 mm. However, Portlandite crystals of such sizes and in such amount as in samples Nos. 1 and 2 do not occur, and the margin is quite often not pronounced (though, this is not completely confirmed by diffractometry but can be attributed to hydrophobic properties of concrete).

### CONCLUSIONS

Addition of surfactant into the composition of gas-concrete mixture and application of fine ground mixture result in significant plasticization of concrete mixture with subsequent decrease in water-to-solid ratio for obtaining of preset plasticity of gas-concrete mixture. In addition, surfactant significantly intensifies structure formation. At the same time, addition of oil sludge as hydrophobic agent leads to certain deceleration of increase in plastic strength. Nevertheless, hydrophobic properties are improved after addition of oil sludge. The studies revealed that structure formation and increase in plastic strength can be adjusted by varying the ratio between the components of complex additive. In the course of the studies another positive property was discovered stipulated by application of the additives. Increase in plastic strength of cellular concrete occurs more intensively, thus intensifying structure formation. Therefore, it is possible to fabricate aerated concrete with fine and uniformly distributed pores of spherical shape, characterized by high strength, lower heat conductance, improved hydrophobic properties and increased frost resistance.

### REFERENCES

- [1] Baranov A. T., Bakhtiyarov K. I., and Ukhov T. A., et al.. Influence of Quality of Macroporous Structure of Cellular Concrete on its Strength and Frost Resistance // Aspects of Cellular Concretes and Structures Thereof. Ed. by A. B. Taranov and V. V. Makarichev. NIIZhB, Moscow, 1972
- [2] S. S. Uderbayev, K. A. Bissenov. Development of a New Method of Aggregate Treatment in the Technology of Lightweight Concrete–Wood Concrete // Mediterranean Journal of Social Sciences MCSER Publishing, Rome-Italy, Vol 5 No 20, September 2014. - P. 2682-2686.
- [3] K.A. Bissenov, S.S. Uderbayev/Research and Development of a New Electromechanochemical Method for the Activation of Mineral Binders // Mediterranean Journal of Social Sciences MCSER Publishing, Rome-Italy, Vol 5 No 20, September 2014. - P. 2711-2716.
- [4] Bisenov K. A. Resource saving technology of monolith foamed concrete on the basis of barchans sands // Zhilishchnoe Stroitel., 1995.-No. 7.- pp.18-20
- [5] Shakhova L.D. and Palalane Zh.A. Selection of sands for production of heat insulating foamed concretes / Tekhnol. Betonov. – 2014. - No. 4. – pp. 12-13
- [6] Merkin A. P. and Zeifman M. I. Optimization of sand particle distribution of engineering cellular concretes // Beton Zhelezobeton. – 1981. - No. 12. - pp. 11-15.
- [7] Mitina, Natalia Aleksandrovna. Obtaining of strong non-autoclave foamed concrete by adjustment of composition and properties of initial blends: Candidate thesis: 05.17.11 Tomsk, 2003.
- [8] Efimenko A. Z., Petrov K. G., and Drozd P. A. Mixing of dry components with aluminum powder and its influence on quality of foamed concrete / Tekhnol. Betonov. – 2014. - No. 8. – pp.36-37.
- [9] Lotov V. A. Phase portrait of cement hydration and solidification // Stroitel. Mater. 2002. - No. 2. - pp. 15-17
- [10] Musaev T. S. and Aubakirova B. M. Influence of modifiers on rheological properties of dry constructing mixtures // Improvement of designs and maintenance systems of transport equipment: Proceedings of International R&D Conference, Almaty, 2009.- pp. 23-26.